

On-Surface Synthesis of Single Conjugated Polymer Chains for Single-Molecule Devices

Yuji Okawa, Swapan K. Mandal, Marina Makarova,
Elisseos Verveniotis and Masakazu Aono

Abstract Although single-molecule electronic devices have been of great interest for several decades, the fabrication of practical circuits remains challenging due to the lack of reliable ways to wire individual molecules. On-surface synthesis of single conductive polymer chains will be a key technology to solve this problem. We already found that stimulating a molecular layer of diacetylene compound by the tip of scanning tunneling microscope (STM) could initiate chain polymerization. As a result, we could systematically fabricate a single conjugated polydiacetylene chain at designated positions. Subsequently, we developed a novel method ('chemical soldering') for connecting the conjugated polymer chains to single organic molecules. The connection of two polydiacetylene chains to a single phthalocyanine molecule was demonstrated. Nanoscale characteristics of the connection were also experimentally and theoretically investigated. Here, we briefly review tip-induced chain polymerization and the chemical soldering methods. This work will help to advance single-molecule electronics.

1 Introduction

To go beyond silicon-based complementary metal-oxide semiconductor (CMOS) technology, recent research focused on single-molecule nanoelectronic devices. In these single-molecule devices, the individual molecules function as electronic components such as rectifiers, transistors, switches, or memories. Since the first

Y. Okawa (✉) · S.K. Mandal · M. Makarova · E. Verveniotis · M. Aono
International Center for Materials Nanoarchitectonics (WPI-MANA),
National Institute for Materials Science (NIMS), Tsukuba, Ibaraki 305-0044, Japan
e-mail: OKAWA.Yuji@nims.go.jp

S.K. Mandal
Department of Physics, Visva-Bharati University, Santiniketan 731 235, India

M. Makarova
Institute of Physics, Prague 18200, Czech Republic

substrate, STM and atomic force microscopy (AFM) experiments can be performed at room temperature both in air and in ultra-high vacuum.

Typical STM images of molecular layers of 10,12-nonacosadiynoic acid and 10,12-pentacosadiynoic acid on highly oriented pyrolytic graphite (HOPG) are shown in Figs. 2a and 3a, respectively. In both cases, parallel bright lines are clearly observed, which indicates that the molecules are self-ordered on the substrate. Figure 2b, c shows magnified STM images of 10,12-nonacosadiynoic acid layers on HOPG and molybdenum disulfide (MoS_2) substrates, respectively. In this case, we can resolve individual molecules. From these high-resolution images, we proposed the model of molecular ordering, as shown in the superimposed models in the figure. In this model, the molecules form flat-lying and closely packed straight rows. The rows are arranged so that COOH end groups in one row are opposite to those of a neighboring row [17, 22].

Though all domains have the same structure on HOPG, we found that the arrangement of molecules varies for different domains on MoS_2 . On the former, the

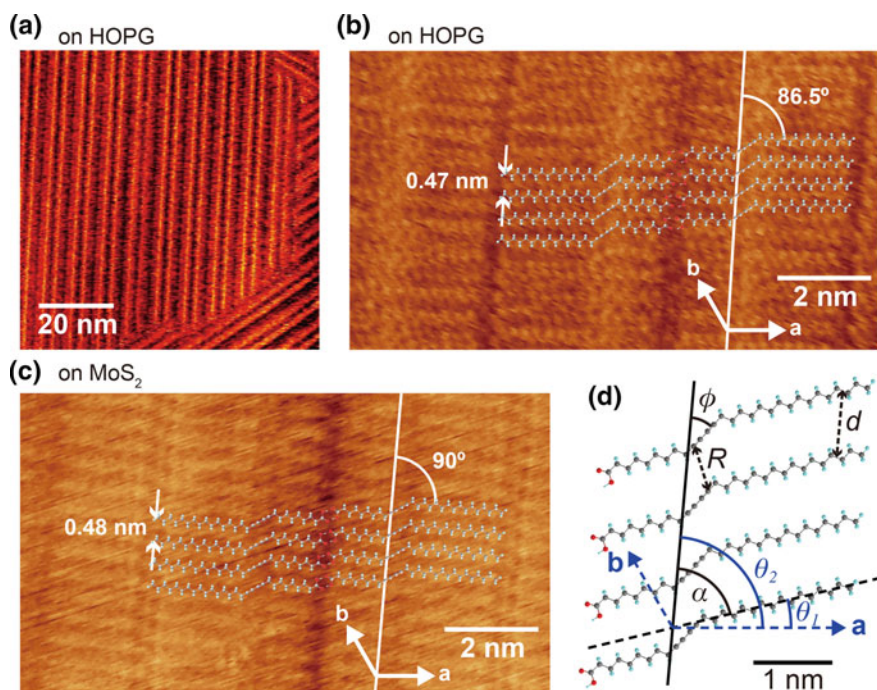


Fig. 2 **a** STM image of a molecular layer of 10,12-nonacosadiynoic acid on a HOPG substrate. **b**, **c** Magnified STM images of the molecular layer on HOPG and MoS_2 substrates, respectively. Molecular models are superimposed in the images. **d** Schematic sketch of the molecular arrangement indicating the structural parameters. Vectors a and b indicate the directions of the underlying substrate lattice. Image **a** adapted from Ref. [19] with permission from The Royal Society of Chemistry. Images **b–d** adapted with permission from Ref. [22]. Copyright 2011, American Chemical Society

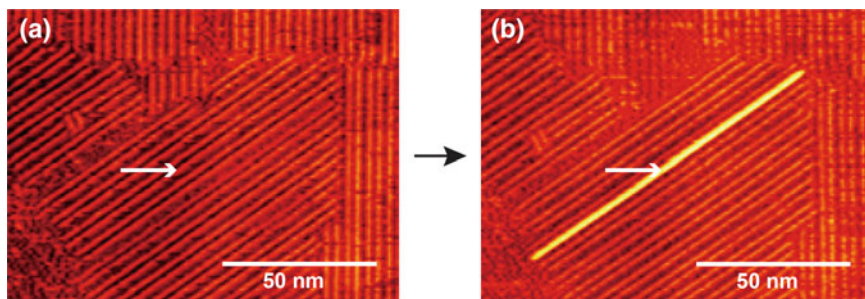


Fig. 3 **a** STM image of a molecular layer of 10,12-pentacosadiynoic acid on a HOPG substrate. **b** STM image of the same area after applying a pulsed sample bias voltage (-4 V in amplitude, 5 μ s in width) at the point indicated by the arrow. The fabricated single polydiacetylene chain is imaged as a *brighter line*. Adapted with permission from Ref. [17]. Copyright 2001, AIP Publishing LLC

orientation of the alkyl side chains is parallel to the main graphite crystal axis. Additionally, the spacing d between neighboring molecules along the direction of the molecular row is always 0.47 nm, and the angle α between the alkyl side chains and the molecular row is 86.5° (see Fig. 2d). On MoS_2 , the angle θ_1 between the alkyl side chains and the main MoS_2 crystal axis varies from -7 to 7° . In this case, the α and d values vary between 85 – 95° and 0.41 – 0.48 nm, respectively [22]. The fluctuation of the molecular arrangement on MoS_2 is probably related to the weaker interactions between the alkyl chains and the MoS_2 , compared to graphite [22].

Tip-induced chain polymerization on a molecular layer of 10,12-pentacosadiynoic acid is shown in Fig. 3. After depositing the layer, we positioned the STM tip over the diacetylene molecule indicated by the arrow, and applied a pulsed sample bias (-4 V in amplitude, 5 μ s in width), as illustrated in Fig. 3a. Figure 3b shows the pulse application product. It reveals a bright line, originating from the point of stimulation. This is a single polydiacetylene chain formed by the tip-induced chain polymerization. Thus, a single straight polydiacetylene chain can be fabricated at any designated position with nm spatial precision. Note that the polymerization is terminated when it encounters a domain boundary (Fig. 3b) [17], a substrate step [23], or an artificial defect [16]. Therefore, when chain polymerization is initiated on larger, defect-free domains, the polydiacetylene chains can be micron-long [24].

3 Lifted-Up Structure of Single Polydiacetylene Chains

Figure 4a shows a typical high-resolution STM image of 10,12-pentacosadiynoic acid monomers and a polymer on a HOPG substrate. A model of the molecular arrangement in the monomer row is depicted in Fig. 4b. We see that the alkyl side chains are oriented parallel to the main graphite crystal axis. Among the

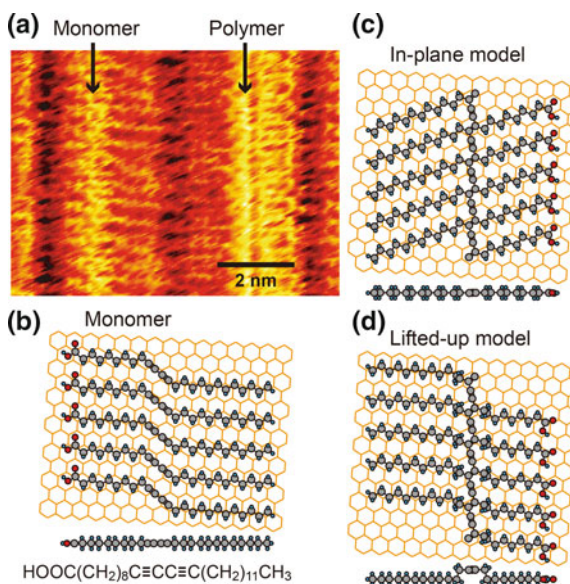


Fig. 4 **a** STM image of a molecular layer of 10,12-pentacosadiynoic acid on a HOPG substrate obtained after ultraviolet irradiation. A photo-polymerized polydiacetylene chain and an unpolymerized monomer row are resolved in the same image. **b** *Top and side* views of the monomer molecular arrangement. **c**, **d** ‘In-plane’ and ‘lifted-up’ conformation models of the polydiacetylene, respectively. Adapted from Ref. [25] with permission from The Royal Society of Chemistry

considerable structure models of the polymer, the simplest one is the ‘in-plane’ structure model (Fig. 4c). In this model, all carbon atoms in the polymer lie in the same plane, parallel to the substrate surface. If this was the case, then, under the experimentally observed condition that the polymer backbone has the same orientation as the linear array of diacetylene monomers, the alkyl side chains should have orientation changes as depicted in Fig. 4c. This is because C–C bonds connecting the alkyl side chains to the polydiacetylene backbone are restricted in directions that satisfy sp^2 and sp^3 bond angles. However, this is inconsistent with STM images such as in Fig. 4a, where orientations of polymer side chains are observed to be parallel to those of monomer side chains. Thus, we proposed a ‘lifted-up’ conformation model (Fig. 4d) [17, 25]. In this model, the alkyl side chains of the polymer are tilted by rotating C–C single bonds which makes the model consistent with the experimental observations. The polydiacetylene backbone is geometrically raised from the level of alkyl side chains.

In first-principles density-functional calculations of the optimized lifted-up structure [25], the height of the polydiacetylene backbone from the alkyl side chains is 0.15 nm. From the total energy calculation, it was suggested that the conformation of the polymer is determined by the stability of an oligomer as an intermediate rather than the stability of a long polymer as a final product. The intermediate oligomer is

restricted between the neighboring monomers which will form chemical bonds with it in the process of chain polymerization. In the case of in-plane structure, the alkyl side chains of the oligomer are not parallel to those of neighboring monomers, thus the alkyl side chains of the oligomer collide with those of the monomers. Hence, the lifted-up oligomer structure is more stable than that of in-plane structure due to the steric hindrance between the alkyl side chains.

The lifted-up structure enables us to observe the single polydiacetylene chains with AFM. In AFM images, the polydiacetylene chains were 0.05–0.16 nm higher than the unpolymerized monomer rows [25], which is consistent with the lifted-up structure model.

Initially, we assumed that only one CH_2 group is lifted at each side of the backbone, symmetrically, as shown in Fig. 4d. However, a recent calculation suggested that the total energy of oligomer could be more stable if one CH_2 group was lifted on one side and two CH_2 groups were lifted on the other side. Further investigations are required to resolve the structure.

4 Reaction Mechanism and Rate-Determining Factors

Figure 5 illustrates the reaction probability P of tip-induced polymerization as a function of applied pulsed sample bias voltage V_s for typical domains of 10,12-nonacosadiynoic acid on HOPG and MoS_2 substrates [22]. The P/V_s dependence is very similar on both substrates. However, the absolute values differ, making the reaction probability on MoS_2 about 4 times higher than that on HOPG. Nevertheless, the similar V_s dependence indicates that the reaction mechanism is the same on both substrates. Furthermore, the plots are nearly symmetric with respect to the polarity of voltage, and the threshold is $\pm 2.7 \pm 0.2$ V on both substrates. This value roughly corresponds to the 3.1 eV energy difference between the diacetylene π - π ground state and the lowest excited π - π^* triplet state [26]. Thus, we can assume that at the first step in chain polymerization, electrons tunneling between the tip and

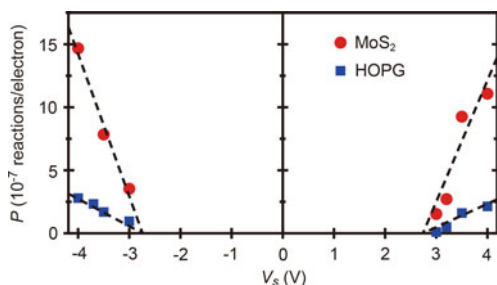


Fig. 5 Plot of tip-induced polymerization rate P per tunneling electron against pulsed sample bias voltage V_s , measured on typical domains of 10,12-nonacosadiynoic acid on HOPG and MoS_2 substrates. Adapted with permission from Ref. [22]. Copyright 2011, American Chemical Society

the substrate pass inelastically through the molecular layer and excite the diacetylene moiety.

This observation is consistent with the process of tip-induced chain polymerization schematically shown in Fig. 6 [17]. This is based on the proposed process for three-dimensional crystals of diacetylene compounds [27]. Initially, a single diacetylene moiety is inelastically excited by tunneling electrons, as described above, creating a reactive diradical state (Fig. 6b). This state has a finite lifetime before relaxing into the underlying substrate. If, within the lifetime of the diradical state, a neighboring diacetylene moiety approaches the diradical via thermal vibrations (Fig. 6c), an addition reaction can take place between them, creating a diacetylene dimer (Fig. 6d). Because the created dimer also has reactive terminals, similar addition reactions can take place on either side. The one-dimensional polymer is thus extended by spontaneously repeating this process along the molecular row (Fig. 6e). During the chain propagation, chain ends have reactive carbenes as illustrated in Fig. 6e.

The greater polymerization reactivity on the MoS₂ substrates can be attributed to the weaker interactions of the alkyl side chains with the MoS₂ compared to graphite. Due to the weaker interaction, molecules on MoS₂ experience more thermal vibrations, which increase the frequency of close-approaching diacetylene moieties favouring dimer formation (Fig. 6c), effectively promoting chain polymerization.

As mentioned above, the arrangement of molecules is always the same on HOPG, but varies in different domains on MoS₂. This structural variation allows us to investigate how the reaction probability is affected by molecular geometry. We determined the structural parameter d and α (Fig. 2d) for each domain from high-resolution STM images such as Fig. 2c. Using these parameters, we then estimated the distance between two reactive carbon atoms that are to be bound by

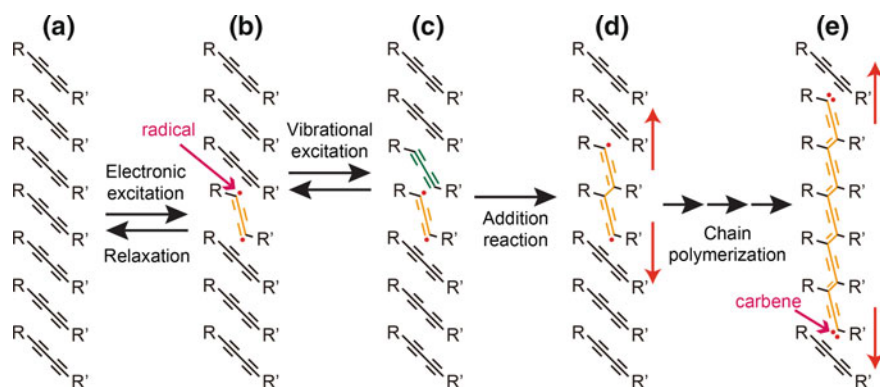


Fig. 6 Illustration of chain polymerization process. **a** Original array of diacetylene compound monomers. **b** A single diacetylene moiety is inelastically excited by tunneling electrons to a reactive diradical state. **c** A neighboring diacetylene moiety approaches one side of the diradical via thermal vibrations. **d** Dimer formation by an addition reaction. **e** Extended polymer formation by chain propagation reaction. The propagating polymer has reactive carbenes at both ends

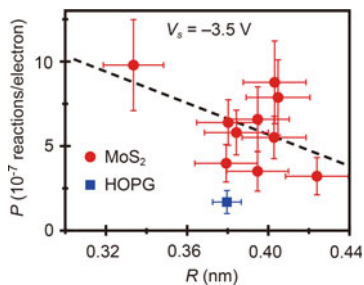


Fig. 7 Plot of tip-induced polymerization rate P per tunneling electron against the reactive carbon-carbon distance, R , for MoS₂ and HOPG substrates. Pulse amplitude V_s and duration were always -3.5 V and 5 μ s, respectively. Adapted with permission from Ref. [22]. Copyright 2011, American Chemical Society

the polymerization reaction, R . This parameter R is a factor of the reaction probability, as seen in the plot in Fig. 7 [22]. This plot indicates that when R decreases by 0.1 nm, the reaction probability P doubles. This is consistent with the reaction mechanism described above. This means that R has a pronounced effect on the occurrence (or not) of the first addition reaction (Fig. 6c, d) within the lifetime of the diradical state.

Recently, we also found that similar molecular layers of diacetylene compound can be formed on a cleaved surface of hexagonal boron nitride (h-BN) nanosheets [28]. H-BN is a layered compound having a similar structure to graphite, except that the two carbon basis set is replaced by boron and nitrogen. It is an insulator with a band gap of 5.97 eV [29]. We found that the photo-polymerization rate on h-BN was approximately 100 times faster than that on graphite. As the band gap of h-BN is larger than the excited energy of diacetylene moiety (5.97 vs. 3.1 eV), the excited state is prevented to relax into the substrate. In contrast, the excited energy can easily relax into graphite or MoS₂. Thus, the excited diradical state (Fig. 6b) has a much longer lifetime on h-BN, resulting in a higher probability of the first addition reaction.

5 Chemical Soldering: New Method for Single-Molecule Wiring

‘Chemical soldering’ is a novel method for connecting conjugated polymer chains to individual organic molecules [18, 19]. The concept is illustrated in Fig. 8. Initially, a target functional molecule is adsorbed on a molecular layer of diacetylene compound. Then, an STM tip is positioned on the same molecular row of the diacetylene compound that the functional molecule is adsorbed, and chain polymerization is initiated as described in Sect. 2. As previously described, the propagating terminals of the chain have the reactive carbenes, as shown in Fig. 6e.

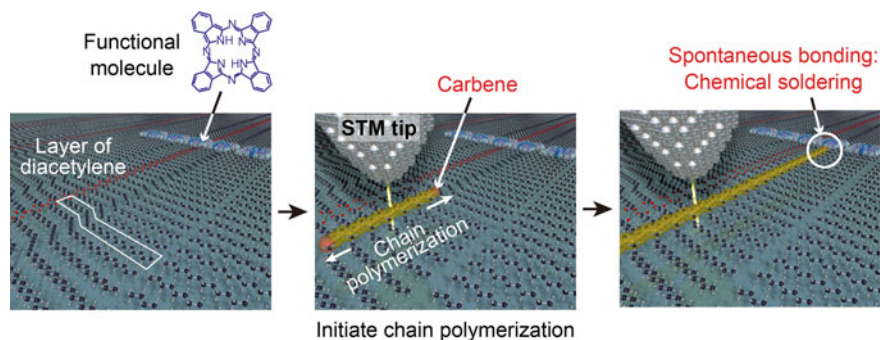


Fig. 8 Illustration of chemical soldering method. After a functional molecule is placed on a molecular layer of diacetylene compound, chain polymerization is initiated using an STM tip. The reactive carbene at the front edge of the chain polymerization spontaneously reacts and bonds with the functional molecule

When the chain polymerization encounters the adsorbed functional molecule, the carbene at the terminal of the polymer reacts not only with a neighboring diacetylene molecule but also with the adsorbed molecule. As a result, a chemical bond is spontaneously formed between the polydiacetylene chain and the target functional molecule. Since the target functional molecule is located above the molecular layer of diacetylene, the lifted-up structure of polydiacetylene is very important for this process, as it enables the reactive carbene to approach the functional molecule.

We initially used phthalocyanine (Pc) as the target functional molecules. They are planar functional dyes with unique electronic and optical properties [30]. Pc molecules are very mobile on HOPG, so it is impossible to observe STM images of isolated Pc molecules at room temperature. However, we found that Pc molecules are stabilized on a molecular layer of 10,12-nonacosadiynoic acid (Fig. 9) [18, 19].

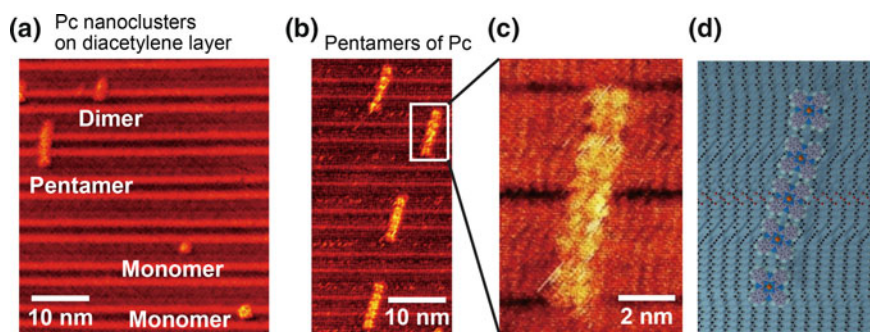


Fig. 9 **a** STM image after depositing a small quantity of copper phthalocyanine molecules on a molecular layer of 10,12-nonacosadiynoic acid lying on HOPG. Monomers, a dimer, and a pentamer of Pc are shown. **b** STM image of Pc pentamers. **c** Magnified STM image of a Pc pentamer. **d** Model of a Pc pentamer. Adapted with permission from Ref. [18]. Copyright 2011, American Chemical Society

In Fig. 9a, the smallest protrusions (labeled ‘monomer’) are isolated single Pc molecules adsorbed above the alkyl side chains of the 10,12-nonacosadiynoic acid molecules. The larger protrusion labeled ‘dimer’ consists of two Pc molecules, and the largest protrusion labeled ‘pentamer’ consists of five Pc molecules, which are shown in Fig. 9b, c. As illustrated in Fig. 9d, a Pc pentamer adsorbs across two rows of 10,12-nonacosadiynoic acid. As the pentamers are frequently observed (Fig. 9b), they most likely represent a stable structure on the molecular layer of 10,12-nonacosadiynoic acid. The first demonstrations of chemical soldering were performed on such pentamers of Pc [18].

Figure 10a shows an STM image of a Pc pentamer adsorbed onto a molecular layer of 10,12-nonacosadiynoic acid on HOPG. Chain polymerization was initiated by applying a pulsed bias voltage to the diacetylene row the Pc was adsorbed onto.

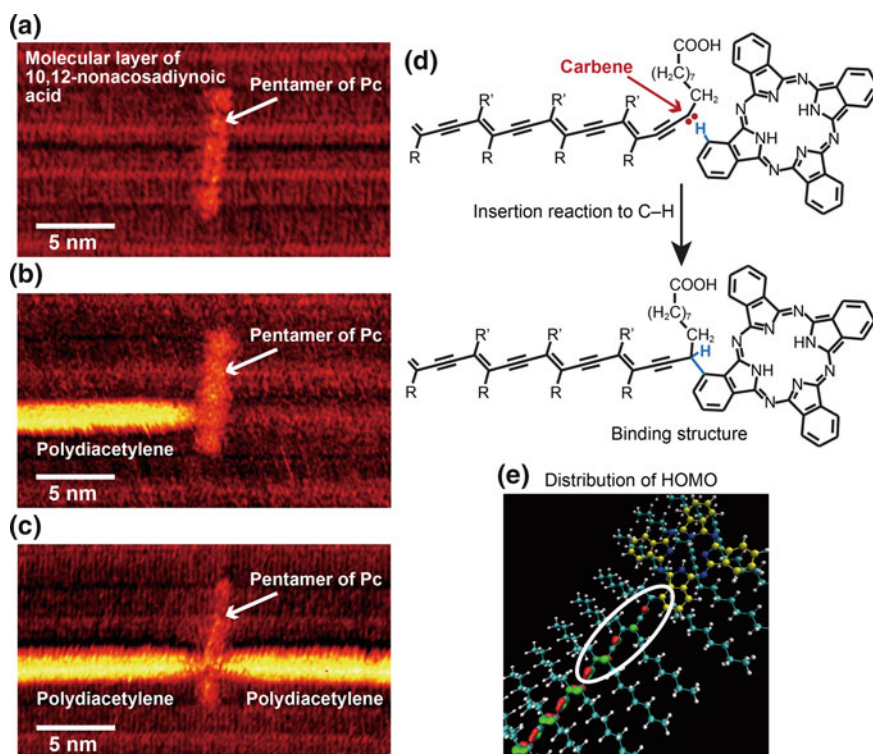


Fig. 10 **a** STM image of a Pc pentamer on a molecular layer of 10,12-nonacosadiynoic acid lying on HOPG. **b** Same area after chain polymerization initiation. A fabricated single polydiacetylene chain (*bright line*) is connected to a Pc molecule. **c** Same area after two polydiacetylene chains are connected to the same Pc molecule. **d** Proposed chemical reaction. The reactive end of polydiacetylene is inserted into a C–H bond of Pc. **e** Optimized structure model for the binding structure. Calculated distribution of HOMO density is also shown. The *white oval* indicates the region of smaller HOMO density. Adapted with permission from Ref. [18]. Copyright 2011, American Chemical Society

As a result, the polydiacetylene chain was connected to the Pc molecule (Fig. 10b). Then, the STM tip was positioned on the other side of the Pc and initiated the second chain polymerization (Fig. 10c), effectively connecting two polydiacetylene chains to the same Pc molecule.

Careful observation of Fig. 10b, c reveals that the image contrast of the polydiacetylene backbone near the Pc connecting point decreased. By repeating similar experiments more than 60 times, we found that approximately 70 % of the images exhibited similar decreased contrast. In the other 30 %, the contrast of the polydiacetylene backbone was relatively unchanged [18]. We considered several possible chemical reactions of the terminal carbene and performed structural optimizations of them [18] via the density-functional first-principles calculations with a wavelet basis set (BigDFT) designed for large-scale calculations [31]. We found that the binding structure, shown in Fig. 10d, e, gives the lowest energy among calculated structures. In this structure, the carbene at the terminal of the polydiacetylene chain is inserted into a C–H bond of Pc, resulting in the formation of chemical bond between them, as shown in Fig. 10d. Figure 10e shows the optimized structure of this binding structure. The calculated density distribution of highest occupied molecular orbital (HOMO) is also depicted in the figure. The calculated HOMO density in the two or three units of the polymer closest to the connecting point (white oval in Fig. 10e) is less than that in the center of the polymer. This is consistent with the decreased contrast in the STM images that reflect the HOMO density. With 70 % of the images showing decreased contrast, we conclude that polymer connection to Pc (chemical soldering) is the main reaction. The remaining 30 % of the images, not exhibiting decreasing contrast, are assigned to a structure where the carbene is inactivated through 1,2-rearrangement of a hydrogen atom, without binding to the Pc.

Concerning the future applications of chemical soldering to Pc, it is suggested that the system where the Pc molecule is connected to two polydiacetylene chains could act as a molecular resonant tunneling diode [18]. As illustrated in Fig. 10d, the terminal carbon atom of the polydiacetylene is converted to sp^3 hybridization by the insertion reaction. Those sp^3 carbon atoms become tunneling barriers between the polydiacetylene and Pc. If the bias voltage is adjusted such that the energy level of the polydiacetylene is equivalent to that of the Pc, then an electron can directly tunnel from the polydiacetylene into the Pc. Thus, electrons can flow from one side to the other through the Pc molecule. If the bias is lower or higher than this voltage, the flow of electrons could be restrained. Such could be a useful component of future single-molecule electronics.

We also succeeded in chemical soldering with fullerene (C_{60}) molecules [32]. When a chain polymerization is initiated to C_{60} nanoislands adsorbed on the molecular layer of 10,12-pentacosadiynoic acid, a cycloaddition reaction occurs between the carbene at the end of polydiacetylene and a single C_{60} molecule. STM observation has proved that the C_{60} molecule is covalently connected to the end of polydiacetylene [32].

6 Summary

In this chapter, we discussed a method for on-surface synthesis of single conjugated polymer chains, using STM tip-induced chain polymerization. This method enables us to fabricate in ambient conditions, single straight polydiacetylene chains at designated positions with nm spatial precision. Using this method, we have proposed and demonstrated ‘chemical soldering,’ for connecting conjugated polymer chains to a single functional molecule. Phthalocyanine and C₆₀ molecules have been used in our demonstrations, but we believe that many other functional molecules can be connected using this method. Thus, this method will be a key technology for the fabrication of single-molecule devices.

Acknowledgments We are grateful to our collaborators, Prof. J.K. Gimzewski (UCLA), Prof. C. Joachim (CNRS), Prof. S. Goedecker (Univ. of Basel), Prof. T. Hasegawa (Waseda Univ.), Dr. C. Hu (Tokyo Univ. of Science), Dr. S. Tsukamoto (Forschungszentrum Jülich and JARA), Dr. D. Takajo (Osaka Univ.), Prof. M. Nakaya (Nagoya Univ.), Dr. Y. Tateyama, Dr. J.P. Hill, Dr. K. Ariga, Dr. T. Taniguchi, and Dr. T. Nakayama (NIMS). This work was supported by World Premier International Research Center Initiative (WPI), the Ministry of Education, Culture, Sports, Science and Technology of Japan (MEXT), and partially supported by JSPS KAKENHI Grant Numbers 21310078 and 24241047.

References

1. Aviram, A., Ratner, M.A.: Molecular rectifiers. *Chem. Phys. Lett.* **29**, 277 (1974)
2. Joachim, C., Gimzewski, J.K., Aviram, A.: Electronics using hybrid-molecular and mono-molecular devices. *Nature* **408**, 541 (2000)
3. Wada, Y., Tsukada, M., Fujihira, M., Matsushige, K., Ogawa, T., Haga, M., Tanaka, S.: Prospects and problems of single molecule information devices. *Jpn. J. Appl. Phys.* **39**, 3835 (2000)
4. Kwok, K.S., Ellenbogen, J.C.: Moletronics: future electronics. *Mater. Today* **5**, 28 (2002)
5. Joachim, C., Ratner, M.A.: Molecular electronics: some views on transport junctions and beyond. *Proc. Natl. Acad. Sci. U.S.A.* **102**, 8801 (2005)
6. Natelson, D., Yu, L.H., Cizek, J.W., Keane, Z.K., Tour, J.M.: Single-molecule transistors: electron transfer in the solid state. *Chem. Phys.* **324**, 267 (2006)
7. Tao, N.J.: Electron transport in molecular junctions. *Nat. Nanotechnol.* **1**, 173 (2006)
8. Choi, H., Mody, C.C.M.: The long history of molecular electronics. *Microelectronics origins of nanotechnology. Social Stud. Sci.* **39**, 11 (2009)
9. Scott, G.D., Natelson, D.: Kondo resonances in molecular devices. *ACS Nano* **4**, 3560 (2010)
10. Song, H., Reed, M.A., Lee, T.: Single molecule electronic devices. *Adv. Mater.* **23**, 1583 (2011)
11. de Ruiter, G., van der Boom, M.E.: Sequential logic and random access memory (RAM): a molecular approach. *J. Mater. Chem.* **21**, 17575 (2011)
12. Fuentes, N., Martín-Lasanta, A., De Cienfuegos, L.Á., Ribagorda, M., Parra, A., Cuerva, J.M.: Organic-based molecular switches for molecular electronics. *Nanoscale* **3**, 4003 (2011)
13. Prauzner-Bechcicki, J.S., Godlewski, S., Szymonski, M.: Atomic- and molecular-scale devices and systems for single-molecule electronics. *Phys. Status Solidi A* **209**, 603 (2012)
14. Pathem, B.K., Claridge, S.A., Zheng, Y.B., Weiss, P.S.: Molecular switches and motors on surfaces. *Annu. Rev. Phys. Chem.* **64**, 605 (2013)

15. Ratner, M.: A brief history of molecular electronics. *Nat. Nanotechnol.* **8**, 378 (2013)
16. Okawa, Y., Aono, M.: Nanoscale control of chain polymerization. *Nature* **409**, 683 (2001)
17. Okawa, Y., Aono, M.: Linear chain polymerization initiated by a scanning tunneling microscope tip at designated positions. *J. Chem. Phys.* **115**, 2317 (2001)
18. Okawa, Y., Mandal, S.K., Hu, C., Tateyama, Y., Goedecker, S., Tsukamoto, S., Hasegawa, T., Gimzewski, J.K., Aono, M.: Chemical wiring and soldering toward all-molecule electronic circuitry. *J. Am. Chem. Soc.* **133**, 8227 (2011)
19. Okawa, Y., Akai-Kasaya, M., Kuwahara, Y., Mandal, S.K., Aono, M.: Controlled chain polymerisation and chemical soldering for single-molecule electronics. *Nanoscale* **4**, 3013 (2012)
20. Wegner, G.: Topochemical polymerization of monomers with conjugated triple bonds. *Macromol. Chem. Phys.* **154**, 35 (1972)
21. Tieke, B., Lieser, G., Wegner, G.: Polymerization of diacetylenes in multilayers. *J. Polym. Sci. Pol. Chem.* **17**, 1631 (1979)
22. Mandal, S.K., Okawa, Y., Hasegawa, T., Aono, M.: Rate-determining factors in the chain polymerization of molecules initiated by local single-molecule excitation. *ACS Nano* **5**, 2779 (2011)
23. Sullivan, S.P., Schnieders, A., Mbugua, S.K., Beebe Jr, T.P.: Controlled polymerization of substituted diacetylene self-organized monolayers confined in molecule corrals. *Langmuir* **21**, 1322 (2005)
24. Takajo, D., Okawa, Y., Hasegawa, T., Aono, M.: Chain polymerization of diacetylene compound multilayer films on the topmost surface initiated by a scanning tunneling microscope tip. *Langmuir* **23**, 5247 (2007)
25. Okawa, Y., Takajo, D., Tsukamoto, S., Hasegawa, T., Aono, M.: Atomic force microscopy and theoretical investigation of the lifted-up conformation of polydiacetylene on a graphite substrate. *Soft Matter* **4**, 1041 (2008)
26. Bertault, M., Fave, J.L., Schott, M.: The lowest triplet state of a diacetylene. *Chem. Phys. Lett.* **62**, 161 (1979)
27. Neumann, W., Sixl, H.: The mechanism of the low temperature polymerization reaction in diacetylene crystals. *Chem. Phys.* **58**, 303 (1981)
28. Makarova, M., Okawa, Y., Verveniotis, E., Taniguchi, T., Joachim, C., Aono, M.: Self-assembled diacetylene molecular wires polymerization on an insulating hexagonal boron nitride (0001) surface. (in preparation)
29. Watanabe, K., Taniguchi, T., Kanda, H.: Direct-bandgap properties and evidence for ultraviolet lasing of hexagonal boron nitride single crystal. *Nat. Mater.* **3**, 404 (2004)
30. de la Torre, G., Claessens, C.G., Torres, T.: Phthalocyanines: old dyes, new materials. Putting color in nanotechnology. *Chem. Commun.* 2000 (2007)
31. Genovese, L., Neelov, A., Goedecker, S., Deutsch, T., Ghasemi, S.A., Willand, A., Caliste, D., Zilberberg, O., Rayson, M., Bergman, A., Schneider, R.: Daubechies wavelets as a basis set for density functional pseudopotential calculations. *J. Chem. Phys.* **129**, 014109 (2008)
32. Nakaya, M., Okawa, Y., Joachim, C., Aono, M., Nakayama, T.: Nanojunction between fullerene and one-dimensional conductive polymer on solid surfaces. *ACS Nano* **8**, 12259 (2014)